Reaction Chemistry & Engineering

Linking fundamental chemistry and engineering to create scalable, efficient processes

Accepted Manuscript

This article can be cited before page numbers have been issued, to do this please use: D. Dhiman, A. S. C. Marques, A. P. M. P. M. Tavares, M. G. Freire and P. Venkatesu, *React. Chem. Eng.*, 2026, DOI: 10.1039/D6RE00047A.

ROYAL SOCIETY OF CHEMISTRY

rsc.li/reaction-engineering

View Article Online
DOI: 10.1039/D6RE00047A

ARTICLE

Superior performance of ionic liquids over deep eutectic solvents in stabilizing L-Asparaginase for sustainable biopharmaceutical applications

Received 00th January 20xx,
Accepted 00th January 20xx

DOI: 10.1039/x0xx00000x

Diksha Dhiman[a,†], Ana S. C. Marques[b,†], Ana P. M. Tavares[b], Mara G. Freire[b]* and Pannuru Venkatesu[a]*

The stability of protein-based biopharmaceuticals is a critical factor limiting their formulation, storage, and clinical performance. This work shows the performance of cholinium-based ionic liquids (ILs) versus deep eutectic solvents (DESs) as sustainable stabilizing agents for L-asparaginase (L-ASNase), a therapeutic enzyme used in the treatment of leukemia. Three cholinium-based ILs, namely cholinium chloride ([Ch]Cl), cholinium bicarbonate ([Ch][HCO_3]), and cholinium glycolate ([Ch][Gly]), and two analogous DESs, namely [Ch]Cl-Glycerol and [Ch]Cl-Glycolic acid (GA), were investigated. These were applied in a range of concentrations (0-80 wt %) to determine their effectiveness in enhancing the enzyme stability and activity. Alterations in both the structure and activity of L-ASNase were observed in response to the hydration content of ILs and DESs, using several spectroscopic and computational techniques, with optimal performance observed at 40 wt %. Notably, [Ch]Cl, [Ch]Cl-Glycerol and [Ch][HCO_3] revealed as promising to be incorporated into ASNase formulations, with [Ch]Cl-Glycerol exhibiting enhanced molecular polarity and establishing extended hydrogen bonding with the protein. On the other hand, both GA and [Ch]Cl-GA lead to the protein loss of stability. The most promising formulations, with ILs and DESs at 40 wt %, were evaluated under different temperature conditions (25 °C and 4 °C), for 5 h and 10 days. The best results were achieved with [Ch]Cl, which significantly enhanced the conformational and colloidal stability of L-ASNase, and with the thermal stability being remarkably increased by 9 °C. Reconstituted L-ASNase can be stored for up to 5 days at 4 °C in aqueous solutions of [Ch]Cl (40 wt %), offering potential cost savings and improved treatment administration. Furthermore, the structure and size of L-ASNase were maintained for at least 3 h at room temperature. Although it depends on the protein under study and conditions investigated, the set of results shown in this work demonstrate that ILs perform as better stabilizers of the ASNase biopharmaceutical than equivalent DESs. Our findings show the potential of cholinium-based formulations in extending the stability and improving the activity of L-ASNase, paving the way for sustainable solutions in the biopharmaceutical sector.

Introduction

Enzymes, distinguished as a specialized class of proteins, exhibit the intrinsic capability to catalyze or accelerate biochemical reactions within biological organisms. Over recent decades, the discovery of innovative and efficacious biocatalysts for diverse applications has captured significant attention from both academic and industrial sectors.[1] Despite these achievements, a common challenge faced by enzymes is the need to maintain or enhance their stability and activity, which is a critical challenge when addressing their use as biopharmaceuticals.[2] L-asparaginase (L-ASNase) holds significant importance in leukemia treatment, being commercially sourced from both *Escherichia coli* and *Erwinia chrysanthemi*, obtained by recombinant technology.[3] The *E. coli*-derived L-ASNase is distributed as a preservative-free lyophilized powder in single-use vials, each containing 10,000 units for injection.[4] Manufacturers recommend storing the reconstituted solution within the temperature range of 2–8 °C and discarding it after eight hours.[5] In this regard, the pharmaceutical industry has expressed specific concerns regarding the potential aggregation and denaturation of L-ASNase during cold storage and the constrained dosage timeframe.[6] Accordingly, there is a critical demand for the development of more stable formulation of L-ASNase.

Recent studies indicate that well-designed ionic liquids (ILs) and deep eutectic solvents (DESs) can serve as effective biomolecule stabilizers, offering notable advantages and enhancements in the stability and activity of proteins and enzymes.[7-9] ILs are constituted by an organic large cation combined with an organic or inorganic anion, while DESs are a combination of at least two compounds, a hydrogen bond acceptor (HBA) and a hydrogen bond donor (HBD).[10,11] Both ILs and DESs can acts as a vast array of potential stabilizers due to the abundance of suitable starting

[a] Department of Chemistry, University of Delhi, Delhi-110 007, India.
[b] CICECO-Aveiro Institute of Materials, Department of Chemistry, University of Aveiro, 3810-193 Aveiro, Portugal.
† These authors contributed equally.
Supplementary Information available: [details of any supplementary information available should be included here]. See DOI: 10.1039/x0xx00000x

materials and their possible combinations.[12,13] The properties of ILs and DESs are strongly determined by the intermolecular interactions they can establish, including Coulomb forces, hydrogen bonding, and dispersion forces. ILs are characterized by dominant ionic interactions (Coulomb forces), while DESs exhibit a strong contribution from hydrogen bonding.[12,14] Despite their shared features of low vapor pressure and a broad liquid range, generalizations regarding toxicity, stability, biodegradability, flammability, and green character are challenging due to their diversity.[7,15]

Apart from these characteristics, promising alternatives for protein/enzyme stabilization have emerged with ILs and DESs as solvents or co-solvents.[8] Recent advancements in using ILs and DESs for stabilizing proteins and enzymes have been recently reviewed.[7,16] Cholinium-based formulations stand out for their eco-friendly nature and are extensively studied for enzyme stability and activity.[7] In this regard, Nascimento *et al.*[17] investigated the stability and activity of *Aspergillus niger* lipase in cholinium-based ILs. The study revealed sustained or increased lipase catalytic activity at lower IL concentrations (<0.1 M), with cholinium acetate ([Ch][Ac]), and suppressed activity at higher concentrations (>0.1 M) with cholinium pentanoate ([Ch][Pent]) and cholinium hexanoate ([Ch][Hex]).[17] Magri *et al.*[18] evaluated the enzymatic activity of commercial L-asparaginase (L-ASNase) in aqueous cholinium-based IL solutions, noting significant activity increases, though higher temperatures negatively impacted activity.[18] Recent studies showed the use of DESs as cosolvents, incorporating small amounts of water to enhance enzyme solubility and stability across various applications.[8,14] Ma *et al.*[19] explored cholinium chloride – ethylene glycol ([Ch]Cl-EtG) for β-glucosidase, achieving a 96% increase in enzyme half-time and 54% rise in ginsenoside compound K yield. Miranda-Molina *et al.*[20], assessed DESs for Thermotoga maritima amylase, finding positive effects in aqueous DES solutions with [Ch]Cl and various HBDs.[20]

In this work, we undertook the evaluation and comparison of the stabilizing capabilities of cholinium-based ILs and equivalent DESs for the prominent anti-leukemia enzyme L-ASNase.[21] This study aims to shed light on the comparative effectiveness of cholinium-based ILs and DESs as stabilizing agents for L-ASNase, providing valuable insights for enhancing enzyme stability and addressing suitable and sustainable formulations for the pharmaceutical industry. For this, the conformational (UV absorption, Fluorescence emission, Far-UV CD, Fourier-transform infrared (FTIR)), thermal and dispersion stabilities (Dynamic light scattering (DLS), CB-DOCK and enzymatic activity of L-ASNase were determined in the presence of three cholinium-based ILs, namely cholinium chloride ([Ch]Cl), cholinium bicarbonate ([Ch][HCO_3]), and cholinium glycolate ([Ch][Gly]), and two cholinium-based DESs, namely cholinium chloride-glycerol ([Ch]Cl-Glycerol), and cholinium chloride-glycolic acid ([Ch]Cl-GA). Both ILs and DESs were investigated at different concentrations (20, 40, 60 and 80 wt %) in water. The enzyme stability in the presence of the individual components was also evaluated. The L-ASNase stability was determined at different temperatures and times, in the presence of the most promising cholinium-based ILs and cholinium-based DESs at 40 wt %, at 25 °C and 4 °C, for 5 h and 10 days. Finally, molecular docking studies were used to address the main interactions between L-ASNase and all five formulations.

Results and Discussion

Effect of cholinium-based formulations on the stability and activity of L-ASNase

Conformational stability. UV-Vis spectroscopy was employed to analyse the solvation environment of L-ASNase aromatic amino acids, specifically focusing on the hydrophobic effect. The complete UV-Vis absorption spectra for the various systems are provided in Figure S1, in the Electronic Supplementary Information (ESI). The maximum absorbance (Amax) of L-ASNase occurs at 280 nm (Figure S1 in the ESI), indicating the capacity of all the formulations to retain the structure of the protein. The second derivative UV-vis spectra ($d^2A/d\lambda^2$) were generated to resolve the change in the signal of the peak centred at 280 nm to extract detailed information about the environment of the protein chromophores (for example, solvent exposure).[22] Figure 1 elucidates the second derivative of the UV-vis absorption spectra of L-ASNase in presence of various cholinium-based formulations.

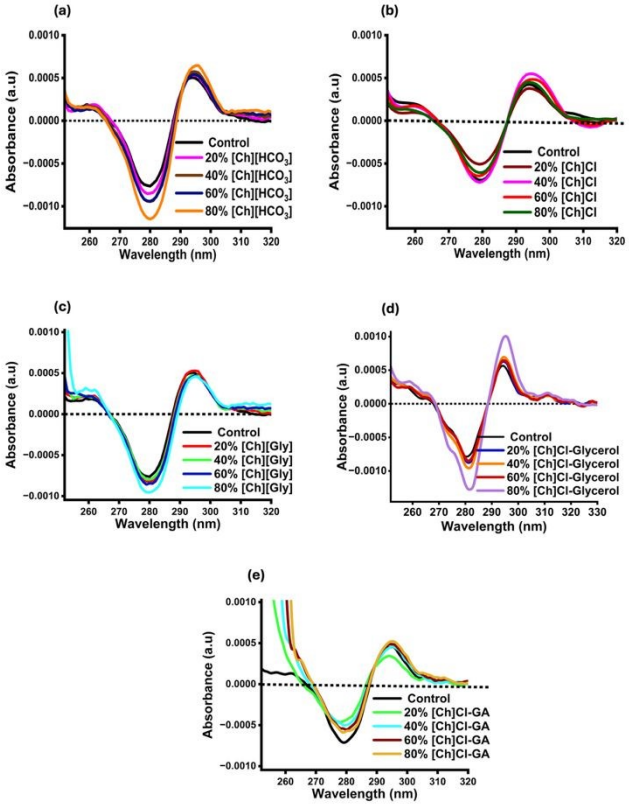

Figure 1. Second-derivative UV-visible absorption spectra of L-ASNase in formulations of various concentrations of (a) [Ch][HCO_3], (b) [Ch]Cl, (c) [Ch][Gly], (d) [Ch]Cl-Glycerol and (e) [Ch]Cl-GA. Control - reference spectrum.

View Article Online
DOI: 10.1039/D6RE00047A

All the formulations kept the retainment of Tyr (287 nm) and Trp (295 nm). However, in the presence of the [Ch]Cl-Glycerol DES, the characteristic absorbance of L-ASNase gradually increases with the increase in the DES concentration. Similar features were observed by L-ASNase in the aqueous solutions of [Ch][HCO_3]. On the other hand, the absorbance spectrum of L-ASNase does not show a direct relation with hydration (%) when using [Ch]Cl, [Ch][Gly] and [Ch]Cl-GA. Interestingly, L-ASNase illustrates a relevant decrease in the absorbance and bathochromic shift in the solutions of [Ch]Cl-GA at 20, 40, 60 and 80 wt %, which relates to the exposure of the aromatic residues of L-ASNase to the more polar environment of the formulation.[23] All characteristic peaks of L-ASNase were preserved in aqueous Gly solutions, while notable disruption occurred in GA (Figure S1 in the ESI), which could be ascribed to the protein denaturation in the extremely acidic conditions provided by GA.[18]

Trp, Tyr and phenylalanine (Phe), the fluorescence probes of L-ASNase, were examined to study additional intermolecular interactions between L-ASNase and cholinium-based formulations. The fluorescence spectra, at an excitation of 280 nm and emission from 300 to 500 nm, were acquired for L-ASNase in PBS (control) and L-ASNase incubated in different cholinium-based formulations (20, 40, 60 and 80 wt %). The corresponding emission fluorescence spectra of L-ASNase in the presence of all cholinium-based formulations are compared with the control in Figure 2.

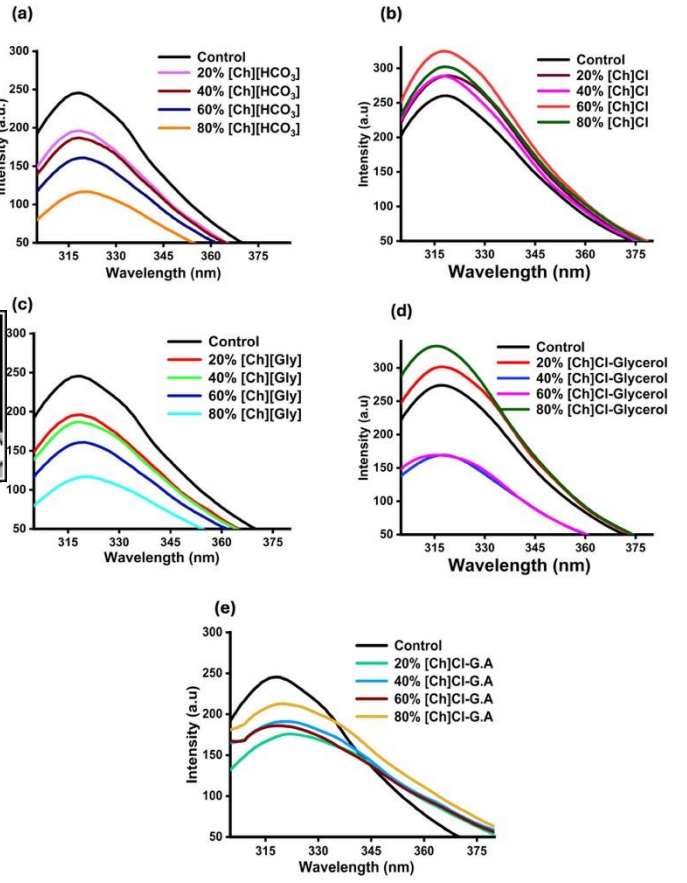

Figure 2. Fluorescence emission spectra of L-ASNase in formulations of (a) [Ch][HCO_3] (b) [Ch]Cl (c) [Ch][Gly], (d) [Ch]Cl-Glycerol and (e) [Ch]Cl-GA at 25 °C and pH =7. Control - reference spectrum.

The fluorescence emission spectra of L-ASNase in the presence of Gly and GA are given in Figure S2 in the ESI. Independent of the type of cholinium-based formulation, the maximum emission intensity (λ_{max}) remained around 319 nm, which is consistent with the reported value.[24] This indicates that the protein remains folded in its native conformation, as previously shown for other protein fluorescence spectrum profiles.[25] However, a slight red shift of L-ASNase (~3 nm) is observed in the presence of [Ch]Cl-GA and GA, likely due to protein denaturation caused by the acidic nature of the solvent systems (Table S10, ESI).

Interestingly, increasing the [Ch]Cl concentration (Figure 2 b) promotes an increase in the fluorescence intensity of the aromatic amino acids present in the L-ASNase structure. This increase in the intensity might be interpreted as an increase in the shielding of hydrophobic residues of L-ASNase from the hydrophilic environment of the solvent system. However, fluorescence quenching of L-ASNase can be seen gradually with [Ch][HCO_3], [Ch][Gly] and [Ch]Cl-GA, and at higher concentrations of [Ch]Cl-Glycerol, which is an indication of decreased hydrophobicity around the fluorophore residues of L-ASNase. Maximum intensity (I_{max}) values of L-ASNase are provided in Table S1 in the ESI.

To ascertain the fluorescence quenching effect, fluorescence quenching of L- ASNase in presence of [Ch][Gly], [Ch][HCO_3] and [Ch]Cl-GA was studied. The Stern–Volmer plot of fluorescence quenching is provided in Figure 3. Generally, in fluorescence spectroscopy, two types of quenching are possible: static quenching or dynamic quenching. In static quenching, a ground state complex forms between fluorophore and quencher, whereas, in dynamic quenching, an excited state collision of fluorophore and quencher takes place. Hence, the quenching ability of [Ch][Gly], [Ch][HCO_3] and [Ch]Cl-GA is predicted with the help of the Stern–Volmer plot which reflects the binding of [HCO_3], [Gly] and GA with L-ASNase in the vicinity of fluorophore and protein backbone. Equation 1 represents the linear relationship between the fluorescence intensity of L-ASNase and the concentration of all three formulations.

$$F_0 / F = 1 + k_{sv}[Q] = 1 + \tau_o k_q [Q] \quad (1)$$

where F_0 is the intensity of the fluorophore in the absence of a quencher; F is the intensity of the fluorophore in the presence of a quencher, and [Q] is the concentration of the quencher.

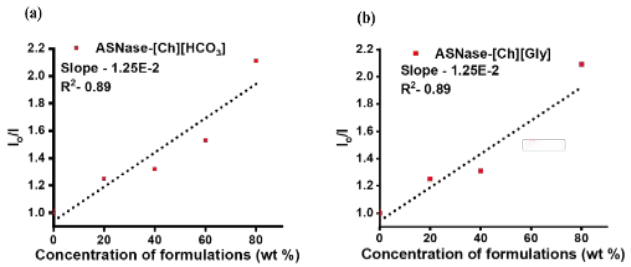

Figure 3. The Stern-Volmer plot of quenching fluorescence emission of L-ASNase in formulation of (a) [Ch][HCO_3] (b) [Ch][Gly] and (c) [Ch]Cl-GA.

View Article Online
DOI: 10.1039/D6RE00047A

k_q is the quenching constant, τ_o is the average lifetime of fluorophore that is 10^{-8}, and k_{sv} is calculated from the slope of F_0/F versus concentration of [Ch][HCO_3], [Ch][Gly] and [Ch]Cl-GA. The k_{sv} values for L-ASNase in presence of [Ch][HCO_3] were obtained from the slope of the Stern–Volmer plot (Figure 3). Due to a very low R^2 value, the Stern-Volmer plot for L-ASNase in the presence of [Ch]Cl-GA is omitted from the figure 3. However, the modest R^2 values for L-ASNase in the presence of [Ch][Gly] and [Ch][HCO_3] attributed to the dual (static and dynamic) quenching mechanism exhibited by the solvent systems. The k_{sv} values were found to be 0.12 M^{-1}. K_q values were obtained from the average lifetime of the fluorophore, with the value 1.25×10^6 s^{-1}. The k_q value was found to be in the order of 10^6 M^{-1} s^{-1} which is less than the maximum dynamic quenching constant value (i.e., 2×10^{10} M^{-1} s^{-1}), thus revealing that fluorescence quenching of L-ASNase in presence of [Ch][HCO_3] arises due to dynamic diffusion. Similarly, both [Ch][Gly] and [Ch]Cl-GA show dynamic quenching with L-ASNase. The obtained K_{sv} and K_q values are provided in Table 1. From these results, it is revealed that [HCO_3] and [Gly] anions, as well as GA, form a complex with the excited Tyr residue of L-ASNase, which is further responsible for its quenching in the fluorescence intensity.

Table 1. Stern−Volmer and Quenching Constant of L-ASNase in the presence of cholinium-based formulations obtained from fluorescence emission experiment at 25 °C (L-ASNase showed increment in emission intensity in [Ch]Cl and [Ch]Cl-Glycerol formulations).

Cholinium-based formulations	K_{sv} / M^{-1}	K_q/ $M^{-1}S^{-1}$
[Ch][HCO_3]	0.12	1.25×10^6
[Ch][Gly]	0.12	1.25×10^6
[Ch]Cl-GA	0.08	8×10^5

Far-CD and FTIR were employed to investigate the secondary structure of L-ASNase in various cholinium-based formulations as a function of concentration. Figure 4 shows the ellipticity of L-ASNase as a function of wavelength, as well as the secondary structure composition (%) of L-ASNase. These were determined using the *dichroweb* software.[26] The values of secondary character of L-ASNase are provided in Table S2, in the ESI. The secondary structure and FTIR spectrum of L-ASNase were also studied in the presence of glycerol and GA, being provided in Figure S2 in the ESI. The far-CD spectrum of native L-ASNase (Figure 4) at 25°C shows two bands at 208 nm and at 222 nm , which correspond to distinct characteristics of the α-helix secondary structure.[27] However, from Figure 4, peaks at 208 and 222 nm of L-ASNase were observed to be deformed when using [Ch][Gly] and [Ch]Cl-GA in the formulations, further showing the perturbation of H-bonding between α-helices of L-ASNase.

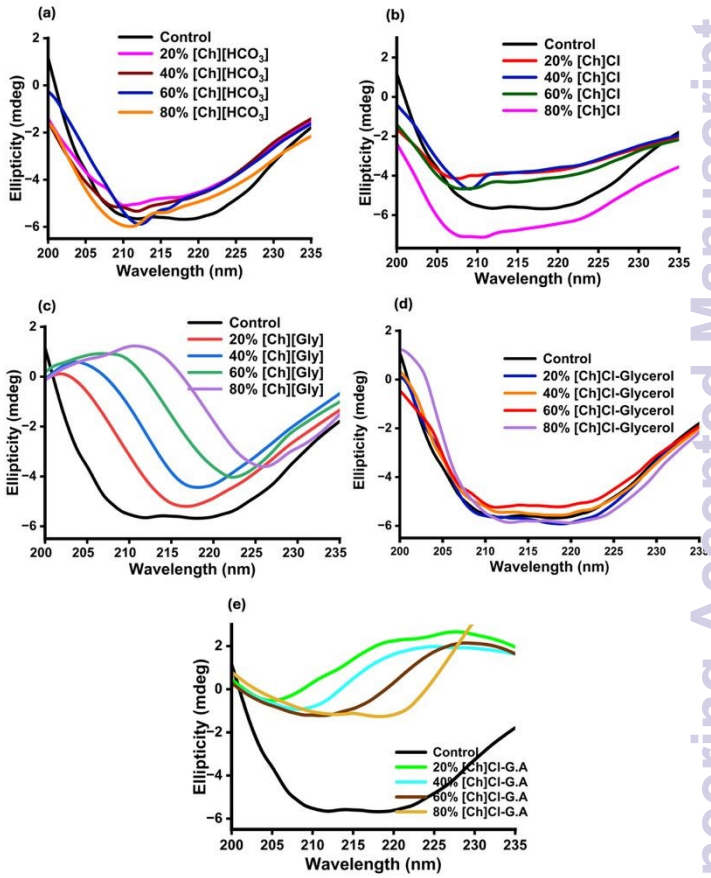

Figure 4. Far-UV CD spectra of L-ASNase in formulations of (a) [Ch][HCO_3], (b) [Ch]Cl, (c) [Ch][Gly], (d) [Ch]Cl-Glycerol and (e) [Ch]Cl-GA. Control - reference spectrum.

Figure 5 illustrates a decrease in the % (α-helix) conformation and an increase in the percentage of the unordered structure of L-ASNase in solutions of [Ch][Gly] and [Ch]Cl-GA. Similarly, in presence of [Ch][HCO_3], negative ellipticity at 208 nm was retained; however, the 222 nm peak gets flattered, being not clearly defined, which can be due to some light exposure of Trp residues to the solvent environment, further indicating some loss of the percentage of the α-helix structure. However, with [Ch]Cl and [Ch]Cl-Glycerol, both peaks stay retained, revealing the higher secondary structure stability of L-ASNase. Therefore, from Far-CD spectroscopy, it can be postulated that the secondary structure of L-ASNase is fully retained with [Ch]Cl and [Ch]Cl-Glycerol aqueous solutions. [Ch][HCO_3] leads to some discrepancy in the L-ASNase peaks; however, this trend can be attributed to extended H-bonding of L-ASNase with the solvent. The vibrational transition mode of the amide I and amide II bonds of L-ASNase was interpreted by FTIR spectroscopy data, in various cholinium-based formulations, to study the effect of formulation polarity (electrostatic interactions) on the L-ASNase secondary structure. Figure 5 shows the measured transmittance spectra of L-ASNase in 40 wt % cholinium-based formulations as a function of the wavenumber. Due to the C=O

View Article Online
DOI: 10.1039/D6RE00047A

stretching vibrations of the peptide bonds, amide I appears in the region of 1625-1695 cm^{-1}, whereas the amide II band is due to C-N stretching vibrations in combination with N-H bending, appearing in the region of 1470-1570 cm^{-1}.[28] From Figure 5 it can be seen that both peaks at 1635 and 1560 cm^{-1} are retained in the presence of all the cholinium-based formulations at 40 wt %. FT-IR spectrum of L-ASNase with [Ch]Cl-GA shows significant noise and, thus, is not included in the final spectrum. Figure 5 illustrates that the highest transmittance of L-ASNase is seen at 1560 cm^{-1}, in presence of [Ch]Cl-Glycerol. The order of L-ASNase transmittance follows the trend: [Ch]Cl-Glycerol > [Ch]Cl > [Ch][HCO_3] > [Ch][Gly] > control. This can be due to extended hydrogen bonding between the N-H bond and cholinium-based formulations. However, the sequence of L-ASNase transmittance at 1635 cm^{-1} reversed, which further reflects the decrease in polarity of the polypeptide backbone of L-ASNase (C=O). [29] This trend is due to the presence of cholinium-based formulations. Overall, the FT-IR spectroscopy results show that the hydrophobic backbone of L-ASNase is shielded in presence of cholinium-based formulations, mostly with [Ch]Cl and [Ch]Cl-Glycerol. However, the FT-IR studies complement the Far-CD results of L-ASNase secondary structure stability, which show the shielding of the polypeptide backbone of L-ASNase in presence of [Ch][HCO_3] with hydrogen bonding in some extent. Overall, the discussed findings suggest that different cholinium-based formulations have varying effects on the conformational

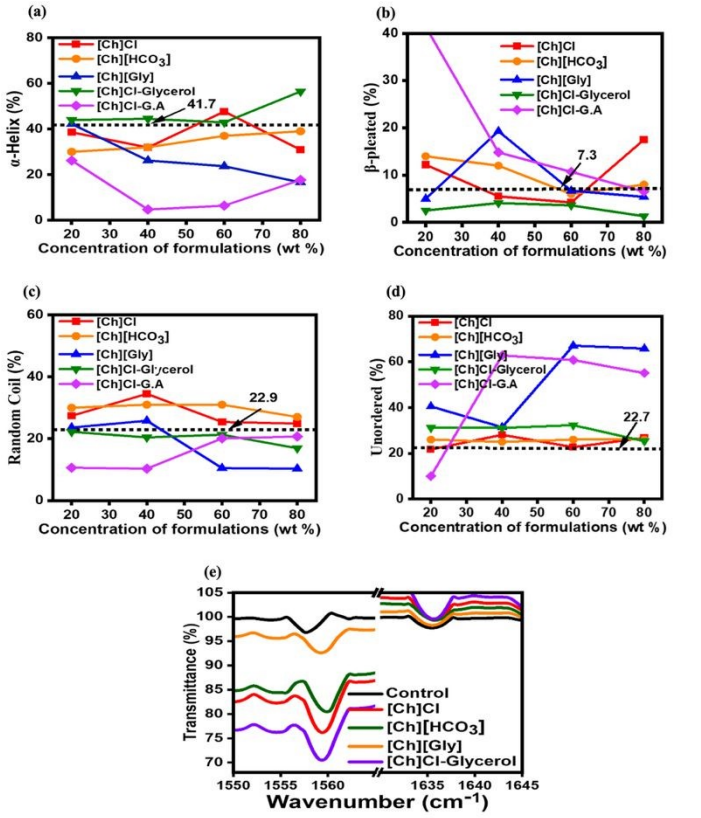

Figure 5. Percentage secondary structure: (a) % α-helix, (b) %β-pleated, (c) % random coil and (d) % unordered structure of L-ASNase in different cholinium-based formulations at 25 °C. (e) FT-IR spectra of L-ASNase in buffer (control; black), [Ch]Cl (red), [Ch][HCO_3] (green), [Ch][Gly] (yellow), [Ch]Cl-Glycerol (purple).

stability of L-ASNase, and in which the IL [Ch]Cl and the DES [Ch]Cl-Glycerol demonstrate the most favourable outcomes in terms of retaining the protein's structural integrity.

Thermal stability. Temperature-dependent fluorescence spectroscopy was employed to examine the shielding potential of the investigated cholinium-based formulations on the thermal denaturation of L-ASNase. The denaturation of L-ASNase was studied using a two-state mechanism. Sigmoidal fluorescence intensity curves as a function of temperature were obtained for L-ASNase in all formulations, being illustrated in Figures S3 and S4 in the ESI. The transition temperature (Tm) values of L-ASNase in all formulations are given in Figure 6, being provided in detail in Table S3, in the ESI.

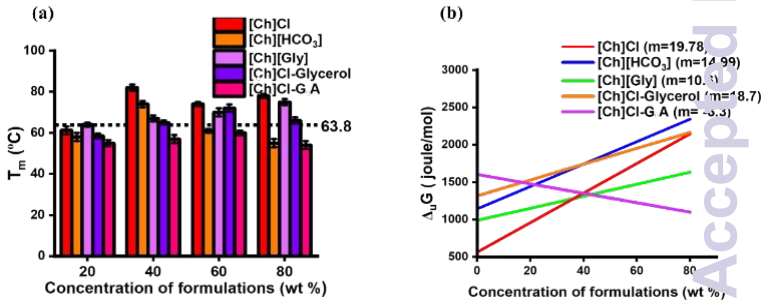

Figure 6. (a) The T_m of L-ASNase as a function of the concentration of cholinium-based formulation. (b) $\Delta_u G$ of L-ASNase as a function of the concentration of cholinium-based formulation.

The T_m of L-ASNase in the buffer is 63.8 °C, agreeing with the literature.[18] Notably, the presence of cholinium-based ionic liquids (ILs) allows superior thermal stability for L-ASNase compared to cholinium-based deep eutectic solvents (DESs). The ascending order of Tm values for L-ASNase (Figures S3 and S4 in the ESI) as a function of solvent content is as follows: for [Ch]Cl, 40 wt% > 80 wt% > 60 wt% > control > 20 wt%; for [Ch]Cl-Glycerol, 60 wt% > 80 wt% = 40 wt% > control > 20 wt%; for [Ch][Gly], 80 wt% > 60 wt% > 40 wt% > 20 wt% > control; for [Ch][HCO_3], 40 wt% > 60 wt% > control > 20 wt% > 80 wt%; and for [Ch]Cl-GA, control > 20 wt% > 40 wt% > 60 wt% > 80 wt%. The thermal stability of L-ASNase does not follow a monotonic trend with [Ch]Cl concentration, revealing competing mechanisms of stabilization and destabilization. As shown in Table S3, the order is 40 wt% > 80 wt% > 60 wt%. The highest T_m at 40 wt% [Ch]Cl represents optimal surface stabilization via cation-π interactions, while the moderately high T_m at 80 wt% suggests a compacted, dehydrated state that resists unfolding.[30] However, at 60 wt%, the reduction in T_m is attributed to either altered hydration or weak chaotropic effects. A similar re-entrant trend is observed for [Ch][HCO_3], which shows a dramatic T_m drop at 80 wt%, indicating chaotropic disruption of the protein's hydrogen bonding network by the bicarbonate anion. In contrast, [Ch][Gly] displays a purely stabilizing trend, with T_m increasing up to 80 wt%, consistent with the 'structure-making' properties of the glycinate anion. The DES systems exhibit distinct behaviors. [Ch]Cl-glycerol shows optimal stabilization at 60 wt%, where the

View Article Online
DOI: 10.1039/D6RE00047A

glycerol component provides preferential hydration while choline chloride maintains surface rigidity.[10] The acidic [Ch]Cl-GA DES produces an unusual plateau where 40 wt% and 80 wt% yield equivalent Tm, attributed to two different destabilization mechanisms: mild acid stress at lower concentrations versus severe crowding-induced aggregation at higher concentrations.[31]

Furthermore, the [Ch]Cl-GA DES leads to the complete denaturation of the protein, not being a good candidate to act as a biopharmaceutical stabilizer of L-ASNase. Insights into the thermodynamic transitions in each cholinium-based formulation were obtained by determining the change in the Gibbs free energy ($\Delta_u G$) of L-ASNase and plotting it as a function of the concentration of cholinium-based formulations. The values of $\Delta_u G$ were calculated from the integral of the Gibbs – Helmholtz equation similar to our earlier studies.[7] Table S4 in the ESI provides the $\Delta_u G$ values of L-ASNase. The influence of different formulations on L-ASNase thermal stability was determined by Equation 2 [32]:

$$\Delta_u G = \Delta G + m\,[c] \qquad (2)$$

where $\Delta_u G$ is the change in Gibbs free energy of the protein in the cholinium-based formulations, [c] is the concentration of the cholinium-based formulation, and *m*-value is determined from experimental data analysis.

$\Delta_u G > \Delta G$ indicates a structure protecting or stabilizing cholinium-based formulation over the protein, whereas $\Delta G > \Delta_u G$ implies the presence of denaturant.[33] Figure 6 shows a positive slope for all the cholinium-based formulations, except for [Ch]Cl-GA that presents a negative slope. The order of *m* is as follows: [Ch]Cl > [Ch]Cl-Glycerol > [Ch][Gly] > [Ch][HCO_3] > [Ch]Cl-GA. Overall, in terms of thermal stability, [Ch]Cl is the best stabilizer identified for L-ASNase, followed by the [Ch]Cl-Glycerol DES.

Dispersion stability. Dynamic light scattering (DLS) was used to investigate the aggregation potential of L-ASNase under

exposure to cholinium-based formulations. The fluctuation in the hydrodynamic diameter (dH) of L-ASNase and mean zeta potential (ζ-potential) is represented in Figure 7. All samples were not filtered to study the insoluble/irreversible aggregation of L-ASNase, thus the dH values provided correspond to the dH of maximum intensity residues.[34] Figure S5 in the ESI further illustrates the L-ASNase spectra in the presence of Gly and GA.

L-ASNase in buffer solution has a d_H of 385 nm, with ζ-potential -of 0.239 mV, at pH 7.0 and 25 °C, being consistent with the literature.[35,36] However, in presence of cholinium-based formulations, the d_H of L-ASNase gradually decreases by decreasing the cholinium-based IL/DES content, reaching a minimum at 20 wt%. Detailed data are provided in Tables S5 and S6 in the ESI. The d_H (nm) order of L-ASNase in presence of cholinium-based formulations at 20 wt % is the following: [Ch][HCO_3] < [Ch]Cl < [Ch][Gly] < control < [Ch]Cl-Glycerol < Gly < [Ch]Cl-GA < GA. Furthermore, at 40 wt %, the sequence is: [Ch]Cl < [Ch][HCO_3] < control < [Ch][Gly] < [Ch]Cl-Glycerol < Gly < [Ch]Cl-GA < GA. Thus, cholinium-based formulations at 20 and 40 wt % lead to a substantial decrease in d_H or to a reduction of the insoluble aggregates of reconstituted L-ASNase.

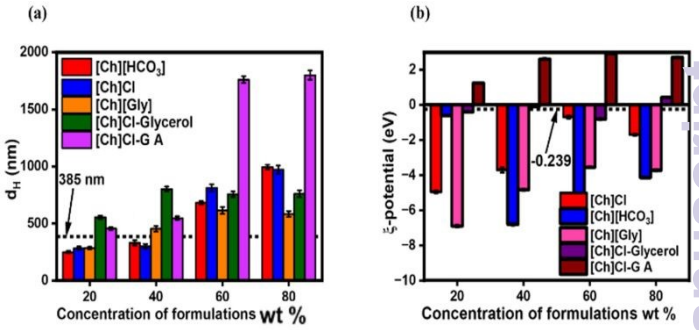

Figure 7. (a) d_H of L-ASNase as a function of the concentration of cholinium-based formulations (0-80 wt) (b) - potential of L-ASNase as a function of the concentration of cholinium-based formulations (0-80 wt) at 25 C (pH=7). Here, the black dashed line represents the d_H and zeta - potential of L-ASNase in the presence of PBS.

Figure 7b elucidates an apparent increase in the ζ- potential of L-ASNase in most cholinium-based formulations, as compared to L-ASNase in buffer, indicating an increase in the electrostatic repulsion between L-ASNase monomers when in presence of cholinium-based formulations. On the contrary, unlike the remaining formulations, L-ASNase exhibits a positive ζ-potential in [Ch]Cl-GA aqueous solutions. This can be ascribed to the acidic nature of the system induced by the GA. Concerning previous studies, at the isoelectric point, proteins generally show a relatively high propensity for aggregation due to elevated hydrophobicity and the absence of inter-repulsive forces.[37] Therefore, based on DLS studies, it can be inferred that the content of cholinium-based components significantly influences the colloidal stability of L-ASNase. Specifically, L-ASNase shows a higher degree of reduction in d_H and an increase in ζ-potential in presence of 20 and 40 wt % of ILs, exhibiting the highest colloidal stability for L-ASNase.

Molecular docking studies. To investigate the preliminary binding affinities and energy landscapes of L-ASNase with ILs and their components, molecular docking studies of L-ASNase were conducted with [Ch]Cl, [Ch][HCO_3], [Ch][Gly], Gly, and GA, using the online software CB-DOCK (Figure 8).[38] Unlike a simple IL that dissociates into free cholinium cations and chloride anions, a DES exists as a supramolecular hydrogen-bonded network with a fixed stoichiometry (1:2 molar ratio of [Ch]Cl to glycerol).[14] Standard molecular docking software (e.g., AutoDock, CB-Dock) is optimized for single, discrete ligands and does not readily accommodate the co-docking of multiple interacting species with variable stoichiometry or the representation of a dynamic supramolecular assembly. The potential interaction between the cavity of the protein and solvent interaction vina score (binding affinity) is provided in Table S8 in the ESI. The order of binding affinity is as follows: [Ch]Cl (- 3.7 Kcal/mol) ≈ [Ch][HCO_3] (-3.7 Kcal/mol) < [Ch][Gly] (-3.9 Kcal/mol) < GA (4.4 Kcal/mol) < Gly (-4.7 Kcal/mol). This indicates that the binding affinity of L-ASNase is the lowest for [Ch]Cl, suggesting these ligands do not

View Article Online
DOI: 10.1039/D5RE00017A

interact favorably with the hydrophobic core of the protein, being a possible reason for the improved stability observed.[37]

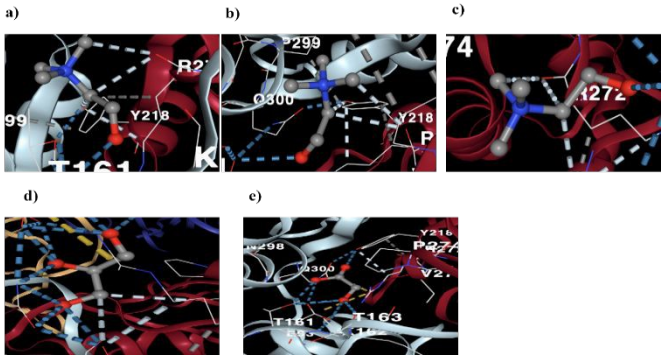

Figure 8. Molecular Docking of L-ASNase using CB-Dock with (a)[Ch][HCO_3], (b)[Ch]Cl, (c) [Ch][Gly], (d) Gly and (e) GA.

Enzymatic activity. Figure 9 shows the L-ASNase activity in the studied cholinium-based formulations, clearly demonstrating a concentration-dependent effect on the catalytic activity of ASNase.

Overall, except for [Ch]Cl-GA, an increasing concentration of both cholinium-based ILs and DESs led to enhanced enzyme activity, comparing with PBS (control). The results obtained for Gly and GA are demonstrated in Figure S6 in the ESI. Based on the results obtained for the 80 wt % of IL and DES, in general, the ILs ([Ch]Cl (220 %), [Ch][HCO_3] (205 %), [Ch][Gly] (167 %)) presented values of higher relative activity when compared to DESs ([Ch]Cl-Glycerol (182 %) and [Ch]Cl-GA (6 %)). Overall, [Ch]Cl led to the highest ASNase activity, with a substantial increase (of ca. 220 %) at 80 wt %. Comparing our findings with existing literature, it is evident that cholinium-based ILs, specifically [Ch]Cl, have a positive impact on L-ASNase activity.[18] While the biocompatibility of cholinium-based formulations contributes to the maintenance of biocatalytic activity, the specific interactions with the protein structure remain unclear. Although the results show that the relative activity of the enzyme is higher in higher concentration formulations (60-80 wt %), the use of lower concentrations (20-40 wt %) is preferable and more convenient when considering biopharmaceutical formulations.[39,40]Therefore, the concentration of 40 wt % was the concentration chosen as the optimal concentration, considering the results of activity and stability. Considering the concentration of 40%, the following relative activity values were recorded for ILs ([Ch]Cl (177%), [Ch][HCO_3] (142%), [Ch][Gly] (151%)) and DESs ([Ch]Cl-Glycerol (138%) and [Ch]Cl-GA (2%)).

According to the literature, the ASNase from *E. coli* was found to be stable in a wide pH range, from 4.5 to 11.5, showing a slight increase in activity and stability in alkaline pHs.[41] The fact that the activity is maximum in alkaline pH is probably due to the balance between L-aspartic acid and L-aspartate.[42] L-aspartic acid in acid pH has a greater affinity for the active site of the enzyme. Under such conditions, it becomes a competitive inhibitor. In alkaline pH, the balance is shifted towards the L-aspartate, which is the form with less affinity to the active site enabling, in this case, a favourable balance for the connection with the substrate L-asparagine.[43] This trend is in line with the results obtained, since, based on the pH values provided in the Table S10 in the ESI, the DES [Ch]Cl-GA has a pH value of 1.6, extremely acidic, thus explaining the possibility why this formulation is completely inhibiting the activity of the enzyme (of ca. 2% of initial activity). This extreme acidity induces conformational changes in the ASNase structure, as it was shown that the secondary structure of the enzyme degraded when pH was smaller than 5.[44-46] Furthermore, it cannot be excluded direct molecular interactions between the [Ch]Cl-GA components and the active site of the enzyme.

On the other hand, the ILs [Ch]Cl, [Ch][HCO_3], [Ch]Gly and the DES [Ch]Cl-Glycerol have pH values that are within the describing range, being beneficial towards the enzyme activity. Overall, considering the results obtained, the IL that leads to the best results is [Ch]Cl, followed by [Ch][HCO_3] and [Ch][Gly], and outperforming the stabilizer effect afforded by DESs.

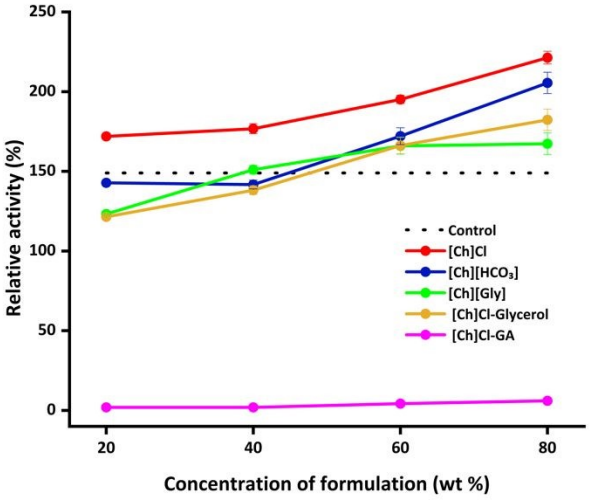

Figure 9. Effect of cholinium-based ILs and DESs concentration in the enzymatic activity of 0.2 mg·mL–1 of ASNase during 15 min: [Ch]Cl (red), [Ch][HCO_3] (blue), [Ch]Gly (green) and cholinium-based DES: [Ch]Cl-Glycerol (orange), [Ch]Cl-GA (pink). The absolute value of 100 % of relative activity corresponds to 149 ± 2.44 U (black dashed line).

Long-term stability of L-ASNase in cholinium-based formulations

Based on the previous results, we exclusively examined further the long-term stability of L-ASNase in the most promising cholinium-based formulations. These include cholinium-based ILs, such as [Ch]Cl, [Ch][HCO_3], and [Ch][Gly], along with the cholinium-based DESs [Ch]Cl-Glycerol. The DES [Ch]Cl-GA was not considered due to its observed destabilizing effect on the enzyme. Furthermore, based on the previously described outcomes, the concentration of 40 wt % was deemed the most promising and was thus employed for assessing the ASNase stability over time. We investigated two different temperatures: 25 °C for a duration of 5 h, and 4 °C for 10 days. These temperature conditions were chosen to mimic

enzyme/biopharmaceutical storage scenarios, with and without refrigeration.

At 25 °C, the Far-CD spectra of L-ASNase show peaks at 222 nm and 208 nm in presence of [Ch]Cl, [Ch][HCO_3] and [Ch]Cl-Glycerol at 40 wt %, being identical to the spectrum of native L-ASNase in the buffer (pH=7) (Figure 10). Despite these promising results, the L-ASNase spectrum shows a shift in presence of [Ch][Gly], revealing the deformation of the secondary structure of L-ASNase. This can be due to relatively higher interaction between the peptide backbone of L-ASNase with the glycolate anion. Overall, at 25 °C, the highest secondary structure stability is achieved after 1 h of exposure of L-ASNase in all cholinium-based formulations.

To further study the potential of cholinium-based formulations on the long-storage of L-ASNase, the samples were stored at -4 °C for 10 days. [Ch]Cl-Glycerol, [Ch][HCO_3] and [Ch]Cl show a higher potential to act as stabilizers as compared to native L-ASNase in buffer. Figure 10 shows that both peaks at 208 and 222 nm were retained after 5 and 10 days when using [Ch]Cl, [Ch][HCO_3] and [Ch]Cl-Glycerol. However, both the peaks got deformed with [Ch][Gly] on day 1, which is in corroboration with earlier studies regarding the enzyme stability.[47]Thus, from Far-CD spectroscopy it can be postulated that the formulations consisting of [Ch]Cl, [Ch][HCO_3] and [Ch]Cl-Glycerol are the ones affording the best storage medium for L-ASNase.

The d_H of L-ASNase was determined, from day 1 to day 10 at 4 °C, to study the aggregation propensity of L-ASNase in cholinium-based formulations. Figure 11 highlights the increase in the size of aggregates of L-ASNase as time proceeds. The order of d_H in day 1 follows the order: [Ch][Gly] (415 nm) > [Ch]Cl-Glycerol (384 nm) > Control (359 nm) > [Ch][HCO_3] (340 nm) > [Ch]Cl (266 nm). In day 10, the order is: Control (1233 nm) > [Ch]Cl-Glycerol (983 nm) > [Ch][Gly] (810 nm) > [Ch]Cl-GA (645 nm) > [Ch]Cl (515 nm) > [Ch][HCO_3] (385 nm).

Thus, from DLS studies it can be interpreted that all the studied cholinium-based formulations perform better than the control. In particular, the ILs [Ch]Cl and [Ch][HCO_3] significantly decrease the aggregation propensity of L-ASNase. Furthermore, from both CD and DLS studies, it is evident that cholinium-based ILs perform better in reducing the L-ASNase aggregation under long-term storage than cholinium-based DESs. Regarding activity assays, the L-ASNase activity in the presence of cholinium-based formulations, at 25 °C and 4 °C (Figure 12), was always higher than the control, demonstrating that these formulations act as strong biocatalytic enhancers. However, the enzymatic activity of L-ASNase decreases with incubation time, especially at 25 °C. This trend allows to conclude that temperature has a relevant influence on the catalytic activity of the enzyme. On decreasing the temperature to 4 °C (Figure 12 b), the addition of cholinium-based formulations was favourable to the L-ASNase activity, allowing to preserve the biocatalytic activity of the enzyme for at least 10 days.

Comparing ILs with the DESs under study, it is notable that the ILs [Ch]Cl, [Ch][HCO_3] and [Ch]Gly are more efficient in stabilizing the enzyme over time than equivalent DESs, for both incubation temperatures. These set of ASNase enzymatic activity experiments demonstrated that it is possible to maintain catalytic activity over time, and even enhance it, using cholinium-based ILs.

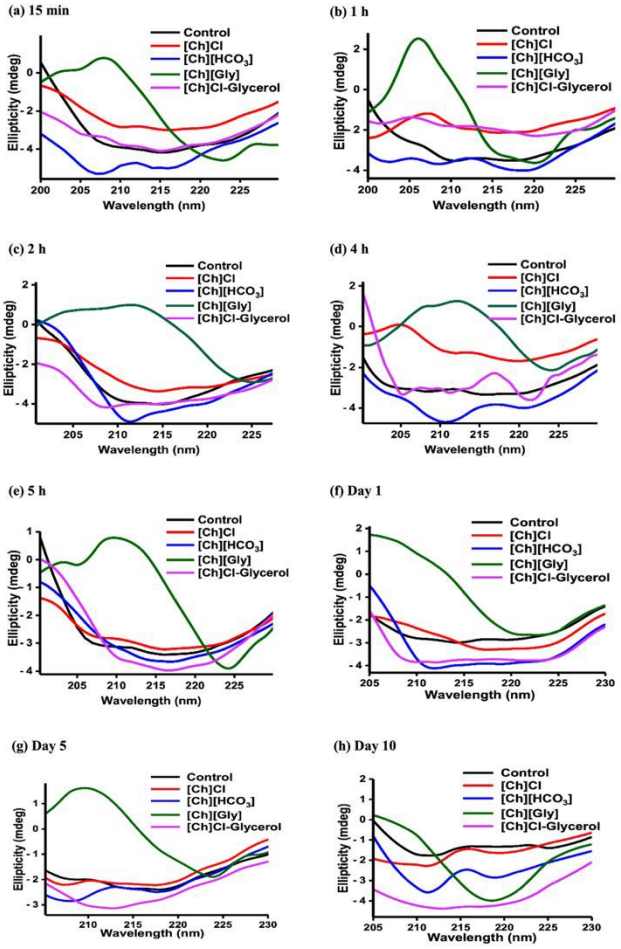

Figure 10. Secondary structure stability of L-ASNase in cholinium-based formulations at 40 wt% as a function of time (a) 15 min, (b) 1 h, (c) 2 h, (d) 4 h, (e) 5 h at 25 °C. Secondary structure stability of L-ASNase in cholinium-based formulations at 40 wt% as a function of time (f), Day 1, (g) Day 5 and (h) Day 10 after storing samples at 4 °C.

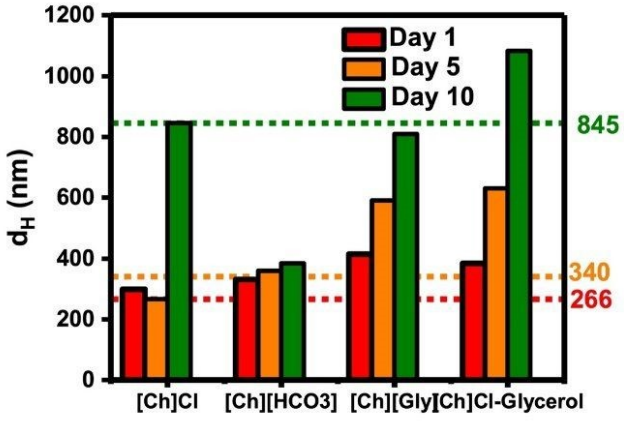

Figure 11. dH of L-ASNase in the presence of different cholinium-based formulations at 40 wt %, 3 straight dotted lines highlight the dH value of L-ASNase in buffer (pH= 7.2 at day 1, day 5 and day 10.

Overall, our results show that the conformational and colloidal stability of L-ASNase is increased in presence of 30-40 wt% of [Ch]Cl (the thermal stability was increased by 9 ˚C), being able to retain its structure and size for over 10 days at 4 ˚C.

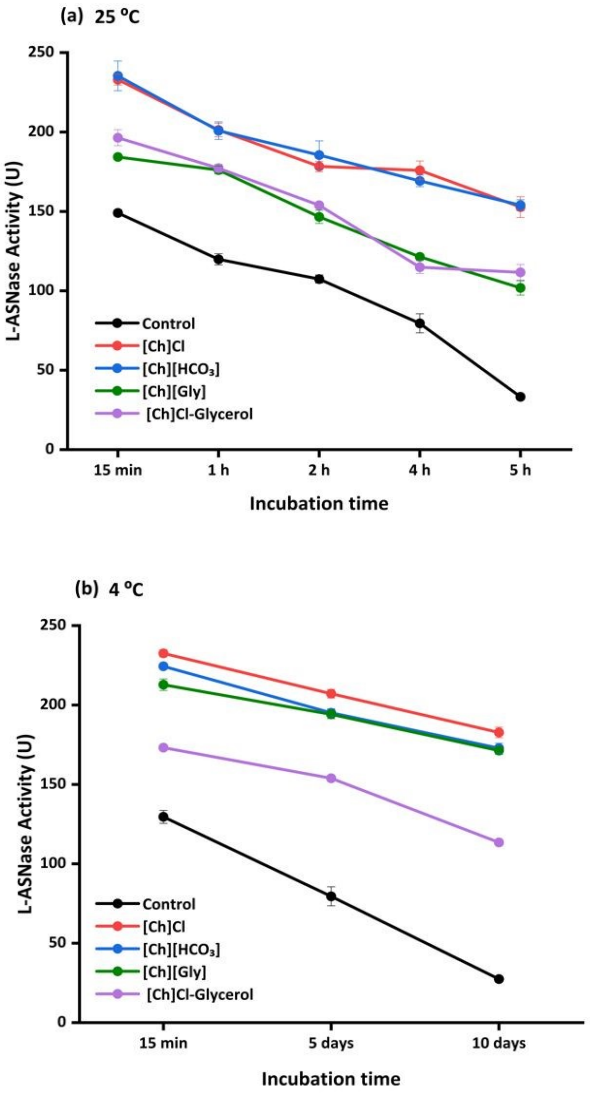

Figure 12. Enzymatic activity of L-ASNase at two temperatures: a) cholinium-based formulations (40 wt %) at 25 °C for 5 h; b) cholinium-based formulations (40 wt %) at 4 °C for 10 days.

Concentrations in the range 30-40 wt % promote the stability of L-ASNase. Similarly, Dicko and co-workers[48] investigated the impact of cholinium-based DESs on three therapeutic proteins noting a trend in hydration with proteins demonstrating the highest stability within the DES range of 20-30 wt %. Further, Bisht *et. al.*[49] have demonstrated that [Ch]-based ILs at lower concentrations can act as an activator for both alpha-chymotrypsin and cytochrome C. Although it depends on the protein under study and conditions investigated, the set of results shown in this work demonstrate that ILs perform as better stabilizers of the ASNase biopharmaceutical than equivalent DESs.

Experimental

View Article Online
DOI: 10.1039/D6RE00047A

Materials and methods

Commercial reagents. The reagents used in the synthesis of cholinium-based ILs and DESs were cholinium chloride ([Ch]Cl, ≥ 98% pure), acquired from Acros Organics-Thermo Fisher Scientific (USA); cholinium bicarbonate ([Ch][HCO_3], 80% in water), glycerol (Gly, ≥ 99% pure) and glycolic acid (GA, 99% pure) provided by Sigma Aldrich (USA); ethyl acetate (≥ 99.5% pure) purchased from Honeywell Research Chemicals- Inc. Fluka (USA); and methanol (≥ 99.9% pure) obtained from Thermo Fisher Scientific (USA). Sodium dihydrogen phosphate (99% pure) and disodium hydrogen phosphate (99.5% pure) were purchased from Sisco Research Laboratories (India). Phosphate Buffered Saline (PBS) was provided by Sigma Aldrich (USA). L-ASNase purified from *E. coli* ASI.357 was purchased, as a lyophilized powder, from ProSpec-Tany TechnoGene Ltd (Israel). To determine L-ASNase activity, the following reagents were applied: L-asparagine (99% pure) purchased from Acros Organics-Thermo Fisher Scientific (USA); Tris(hydroxymethyl) aminomethane (Tris, 99% pure) obtained from Alfa-Thermo Fisher Scientific (Germany); Trichloroacetic acid (TCA, 99.5%) acquired from Sigma-Aldrich-Merck KG. AA (USA); and Nessler's reagent (pure) provided by Carlo Erba Reagents S.A.S. (France). All solutions were prepared in ultrapure water obtained using a Milli-Q plus water purification apparatus.

Synthesis and characterization of cholinium-based ILs. Cholinium glycolate ([Ch][Gly]) was synthesized *via* neutralization of cholinium bicarbonate ([Ch][HCO_3]) with glycolic acid (GA).[50] A slightly excess of GA (dissolved in methanol/water mixture (1:1)) was added drop-wised to [Ch][HCO_3], under ambient conditions (25 °C).The mixture was stirred continuously at 25 °C for 24 h until CO_2 release ceased. The methanol/water mixture was then evaporated under reduced pressure using a rotary evaporator (50 °C, 206 mbar and 42 mbar). Ethyl acetate was added to the synthesized IL to remove the excess of acid. Then, the solvent was removed under reduced pressure using a rotary evaporator (50 °C, 153 mbar). Finally, the IL was dried under vacuum. The chemical structure of the synthesized IL and the respective individual components were confirmed by ^{1}H NMR and FTIR spectroscopy. These data are reported in Figure S7 in the ESI.

Preparation and characterization of cholinium-based DESs. Two DESs, namely [Ch]Cl-Glycerol and [Ch]Cl-Glycolic acid, were prepared. The process involved mixing the HBA ([Ch]Cl) with one HBD (Gly or GA) in 1:2 molar ratios. The mixture was magnetically stirred at 60 °C for 2 h, until a homogeneous liquid was obtained. The chemical structure of the synthesized DESs and their respective individual components were confirmed by ^{1}H NMR and FT-IR spectroscopy. These data are reported in Figure S7 in the ESI. The chemical structures and the respective pH of the cholinium-based formulations studied are shown in Table S10.

View Article Online
DOI: 10.1039/D6RE00047A

Enzymatic Activity of L-ASNase. A stock solution of L-ASNase was prepared at a concentration of 0.4 mg/mL in sodium phosphate buffer, PBS (pH 7, 10 mM). The L-ASNase stability (at a final concentration of 0.2 mg/mL) was determined in the presence of the cholinium-based ILs [Ch]Cl, [Ch][HCO_3] and [Ch][Gly], and the cholinium-based DESs [Ch]Cl-Glycerol and [Ch]Cl-GA, at the following concentrations: 20, 40, 60 and 80 wt %. After homogenization, the samples were incubated at 25 °C for 15 min. The same procedure was performed for PBS and for the cholinium-based DESs individual components: Gly and GA. These formulations were used for the evaluation of conformational, thermal and dispersion stabilities, and enzymatic activity as described below. The results represent the average of three independent experiments ± standard deviation errors.

UV absorption. UV spectra were measured using a Shimadzu UV-1800 (Japan) spectrophotometer with the highest resolution (1 nm) in a wavelength range of 200–350 nm using quartz cells with a path length of 1 cm at 25 °C.

Fluorescence emission. A Cary Eclipse spectrofluorometer from Varian optical spectroscopy instruments (Australia) equipped with a thermostat cell holder was used to monitor the fluorescence emission spectra. The excitation wavelength (λ_{exc}) was set to 275 nm and the emission spectra (λ_{ems}) recorded between 280 to 400 nm to calculate the contribution of the tyrosine (Tyr) and tryptophane (Trp) residue to the overall fluorescence emission.[51] The slit widths for excitation and emission were being set at 5 nm

Far-UV CD. Far-UV CD spectroscopy was carried out using the Jasco J-815 spectrophotometer, with a quartz cuvette of path length 0.1 cm, at 25 °C. The wavelength range was set from 190 to 240 nm at 25 °C. Other fixed parameters correspond to: response time (1 s); bandwidth (1 nm) and scan rate (50 nm/min). The spectrum of PBS buffer alone was taken and deducted from the final scan, functioning as a baseline correction.
For all spectroscopic data Measurements taken on different days may show small variations in peak intensity or position due to instrumental drift. All conclusions rely on solvent-induced changes relative to the same day's reference (Control), not on cross-day reference comparisons.

Fourier-transform infrared (FTIR). FTIR spectra were recorded using an IRAffinity-1S Shimadzu FTIR spectrometer. FTIR spectra were obtained in the wavenumber range of 4000-400 cm^{-1} by accumulating 256 scans, with a resolution of 4 cm^{-1} in transmittance mode. All samples were prepared in a D_2O buffer.

Thermal stability. The samples were incubated from 20 to 90 °C and then analyzed by the fluorescence spectra at an exciting wavelength of 275 nm. Thermal unfolding analyses were conducted using a 1 cm path length cuvette. The temperature was increased at a rate of 2 °C/min using a peltier thermocouple, with a time constant of 16 s. All the unfolding transitions of the L-ASNase were determined by employing the two-state unfolding mechanism.

Dynamic light scattering (DLS). The DLS was of the company Zetasizer Nano instrument (ZS90), (Malvern Instruments Ltd., UK), equipped with He-Ne laser (4 mW, 632.8 nm). The scattering angle was set to 90° with a fixed operating wavelength of 633 nm.[52]

Molecular docking. CB-DOCK online software was used to estimate the probable binding modes of different cholinium-based designer solvents with L-ASNase. L-ASNase structure (PDB ID 6v5f) was downloaded from the protein data bank and the structure was optimized by removing water molecules using PyMol software. The structures of solvents were optimized by PyMol software. Molecular docking was performed by applying CB DOCK.[53]

ASNase Enzymatic Activity Assays. The L-ASNase enzymatic activity was conducted following the protocol adapted from Magri *et al*.[18] Briefly, the quantification of L-ASNase activity involves the quantification of the ammonia released during the hydrolysis reaction of the amino acid L-asparagine. The enzyme assay mixture comprised 50 µL of sample, 450 µL of distilled water, 500 µL of 50 mM Tris-HCl buffer (pH 8.6) and 50 µL of freshly L-asparagine solution (189 mM). The enzymatic reaction was incubated at 37 °C for 30 min, previously defined as the optimal incubation time.[54,55] The linearity of the reaction over 30 min under the described conditions has been verified (Figure S8 in the ESI). After the incubation, the enzymatic reaction was stopped by adding 250 µL of 1.5 M trichloroacetic acid (TCA). Subsequently, the ammonium produced during L-asparagine hydrolysis by L-ASNase, which is directly proportional to L-ASNase activity, was quantified using the Nessler method. For this, 100 µL of the previous sample was added to 2.15 mL of water and 250 µL of Nessler's reagent, followed by a 30 min incubation at room temperature. Then, the absorbance of the sample was measured at 436 nm using a multimode microplate reader (Synergy HT, BioTek, Winooski, VE, USA). A calibration curve (Figure S9 in the ESI) was previously established by reacting Nessler's reagent with ammonium sulphate aqueous solution at various concentrations. The enzyme activity ($A_{L-ASNase}$) was calculated using Equation (3) and is expressed in µmol mL^{-1} min^{-1} (U mL^{-1}).

$$A_{ASNase} = \frac{\mathbf{NH_4^+} \times \mathbf{V_R} \times \mathbf{V_N}}{\mathbf{V_S} \times \mathbf{R_T} \times \mathbf{V_{L-ASNase}}} \quad (3)$$

where NH_4^+ is the ammonium concentration produced in the enzymatic reaction (µmol mL^{-1}), V_R is the volume of enzymatic reaction (1 mL), V_N is the volume of the Nessler reaction (2.5 mL), V_S is the volume of the stopped reaction sample (0.1 mL), R_T is the reaction time (30 min), and $V_{L\text{-}ASNase}$ is the volume of L-ASNase used (50 µL). One unit of L-ASNase activity (U) corresponds to 1 µmol of NH_4^+ produced per minute at pH 8.6 and 37 °C.

View Article Online
DOI: 10.1039/D5RE00047A

The Relative Activity (%) of L-ASNase was calculated according to Equation (4).

$$\text{Relative Activity (\%)} = \frac{\mathbf{A_{sample}}}{\mathbf{A_{initial}}} \quad (4)$$

where A_{sample} and $A_{initial}$ are the L-ASNase activity after the incubation period with different cholinium-based formulations and the initial enzymatic activity, respectively.

Control experiments were performed to evaluate possible interference of ILs and DESs on the enzymatic reaction conditions. The studied ILs and DESs were mixed with buffer solutions without L-ASNase at the same experimental conditions. The enzymatic reaction, and ammonium quantification were performed as described above and no reaction was detected.

Long-term stability of L-ASNase. A stock solution of L-ASNase was prepared at a concentration of 0.4 mg/mL in sodium phosphate buffer, PBS (pH 7, 10 mM). The L-ASNase stability (at a final concentration of 0.2 mg/mL) was determined in the presence of the most promising cholinium-based ILs [Ch]Cl, [Ch][HCO_3] and [Ch][Gly] and cholinium-based DES [Ch]Cl-Glycerol at 40 wt %. The samples were homogenized and incubated at 25 °C and 4 °C for 5 h and 10 days, respectively. Aliquots, from the samples at 25 °C were taken after 15 min, 1, 2, 4 and 5 h. From the samples at 4 °C, aliquots were taken after 1, 5 and 10 days. The results represent the average of three independent experiments ± standard deviation errors.

Conclusions

This work demonstrates the potential of cholinium-based ILs over DES analogues as sustainable and efficient stabilizers of L-asparaginase, a key biopharmaceutical in the treatment of leukemia that currently faces stability concerns associated to formulation and storage. In particular, it is demonstrated that the amino acid environment and secondary structure of L-ASNase stayed intact in presence of [Ch]Cl, [Ch][HCO_3] and [Ch]Cl-Glycerol. On the contrary, FTIR and Far-CD studies illustrate the complete disruption of the secondary structure of L-ASNase in the presence of [Ch][Gly] and [Ch]Cl-GA. Furthermore, molecular docking studies confirmed that [Ch][Gly] has a higher potential to interact with the hydrophobic domain of L-ASNase, thus compromising the enzyme. Colloidal-stability studies of L-ASNase showed that cholinium-based ILs are more efficient in reducing aggregation compared to cholinium-based DESs. The change in the structure and activity of L-ASNase is dependent on the hydration of the ILs or DESs. All the formulations perform best at 40 wt %. In the same line, enzymatic activity assays demonstrate a concentration-dependent effect of cholinium-based formulations, with [Ch]Cl exhibiting the highest activity, followed by [Ch][HCO_3] and [Ch][Gly]. Cholinium-based formulations consistently enhanced L-ASNase activity compared to the control, particularly at lower temperatures. Moreover, [Ch]Cl, [Ch][HCO_3], and [Ch]Gly are more effective in stabilizing the enzyme over time than equivalent DESs, highlighting their potential as robust biocatalytic enhancers for prolonged enzymatic activity.

Overall, through an in-depth comparison using several techniques, it is here shown that ILs outperform DESs in enhancing the conformational, thermal, and colloidal stability of L-ASNase. In particular, [Ch]Cl at 40 wt% significantly increased the enzyme's thermal stability (by 9 °C), maintained its structural integrity for up to 10 days at 4 °C, and enhanced its catalytic activity. These results demonstrate the importance of rational solvent selection, positioning cholinium-based ILs as more effective and sustainable alternatives for the formulation and long-term storage of protein-based biopharmaceuticals.

Author contributions

Diksha Dhiman: Writing – original draft, Writing – review & editing, Methodology, Data Curation, Formal Analysis, Investigation, Validation.

Ana S. C. Marques: Writing – Review, Methodology, Data Curation, Formal Analysis, Investigation, Validation.

Ana P.M. Tavares: Writing – Review & Editing, Conceptualization, Supervision, Resources.

Pannuru Venkatesu: Writing – Review & Editing, Conceptualization, Supervision, Resources, Funding Acquisition, Project Administration.

Mara G. Freire: Writing – Review & Editing, Conceptualization, Supervision, Resources, Funding Acquisition, Project Administration.

Conflicts of interest

There are no conflicts to declare.

Data availability

The data supporting this article have been included as part of the Supplementary Information.

Acknowledgements

P.V. gratefully acknowledge Institute of Eminence (IoE), University of Delhi through Grant No. Ref. No./IoE/2024-25/12/FRP for their financial support. D.D. thanks the Council of Scientific and Industrial Research (CSIR), New Delhi for providing SRF (Senior Research Fellowship). This work was developed within the scope of the project CICECO – Aveiro Institute of Materials, UID/50011/2025 (DOI 10.54499/UID/50011/2025) & LA/P/0006/2020 (DOI 10.54499/LA/P/0006/2020), financed by national funds through the FCT/MCTES (PIDDAC). A.S.C. Marques acknowledges FCT for the PhD grant 2023.04854.BD (DOI 10.54499/2023.04854.BD). A.P.M. Tavares acknowledges the FCT for the research contract CEECIND/2020/01867 (DOI 10.54499/2020.01867).

References

1 P. K. Robinson, *Essays Biochem*, 2015, **59**, 1–41.
2 R. Nag, Srishti J. Anurag, S. Rathore and S. Majumder, *J. Am. Chem. Soc.*, 2023, **145**, 10826–10838.
3 D. I. Marlborough, D. S. Miller and K. A. Cammack, *Biochim Biophys Acta*, 1975, **386**, 576–589.
4 J. Thiman, N. Northrup, C. Saba, D. Clarke, R. Regan, T. Hamilton, H. Lindell and E. Hofmeister, *J Vet Pharmacol Ther*, 2016, **39**, 572–577.
5 ProSpec, L-Asparaginase, https://www.prospecbio.com/l-asparaginase.
6 L. P. Brumano, F. V. S. da Silva, T. A. Costa-Silva, A. C. Apolinário, J. H. P. M. Santos, E. K. Kleingesinds, G. Monteiro, C. de O. Rangel-Yagui, B. Benyahia and A. P. Junior, *Frontiers Bioeng Biotech,* 2019, **6,** 212.
7 S. Shipovskov, H. Q. N. Gunaratne, K. R. Seddon and G. Stephens, *Green Chem.*, 2008, **10**, 806-810.
8 D. Dhiman, A. S. C. Marques, M. Bisht, A. P.M. Tavares and M. G. Freire, *Green Chem.*, 2023, **25**, 650-660.
9 L. Rehmann, E. Ivanova, J. L. Ferguson, H.Q. N. Gunaratne, K. R. Seddon and G. M. Stephens, *Green Chem.*, 2012, **14**, 725-733
10 A. S. Fernandez, S. Prevost and M. Wahlgren, *Green Chem.*, 2022,**24**, 4437-4442.
11 N. Yadav and P. Venkatesu, *Phys. Chem. Chem. Phys.*, 2022, **24**, 13474-13509.
12 J. S. Almeida, E. V Capela, A. M. Loureiro, A. P. M. Tavares and M. G. Freire, *ChemEngineering*, 2022, **6,** 51.
13 T.-X. Yang, L.-Q. Zhao, J. Wang, et al., ACS Sustainable Chem. Eng. 2017, **5**, 5713−5722.
14 D. Dhiman, M. Alhammadi, H. Kim, R. Umapathi, Y. S. Huh, P. Venkatesu, *Adv Therapeutics* 2024, **7**, 2400090.
15 I. Wazeer, M. Hayyan and M. K. Hadj-Kali, *J Chem Technol Biotech*, 2018, **93**, 945–958.
16 N. V. P. Veríssimo, C. U. Mussagy, H. B. S. Bento, J. F. B. Pereira and V. de C. Santos-Ebinuma, *Biotechnol Adv*, 2024, **71**, 108316.
17 P. A. M. Nascimento, J. F. B. Pereira and V. de Carvalho Santos-Ebinuma, *Bioprocess Biosyst Eng*, 2019, **42**, 1235–1246.
18 A. Magri, T. Pecorari, M. M. Pereira, E. M. Cilli, T. L. Greaves and J. F. B. Pereira, *ACS Sustain Chem Eng*, 2019, **7**, 19720–19731.
19 Z. Ma, Y. Mi, X. Han, H. Li, M. Tian, Z. Duan, D. Fan and P. Ma, *Bioprocess Biosyst Eng*, 2020, **43**, 1195–1208.
20 A. Miranda-Molina, W. Xolalpa, S. Strompen, R. Arreola-Barroso, L. Olvera, A. López-Munguía, E. Castillo and G. Saab-Rincon, *Int J Mol Sci*, 2019, **20**, 5439.
21 A. M. Faschinger and N. Sessler, *Adv Ther*, 2019, **36**, 2106–2121.
22 S. Khemaissa, S. Sagan and A. Walrant, *Crystals (Basel)*, 2021, **11**, 1032.
23 R. Ragone, G. Colonna, C. Balestrieri, L. Servillo and G. Irace, *Biochemistry*, 1984, **23**, 1871–1875.
24 J. T. Vivian and P. R. Callis, *Biophys J*, 2001, **80**, 2093–2109.
25 M. R. Eftink and C. A. Ghiron, Biochemistry, 1976, **15,** 672-80.
26 A. J. Miles, S. G. Ramalli and B. A. Wallace, *Protein Sci*, 2022, **31**, 37–46.
27 A. Pabbathi and A. Samanta, *J Phys Chem B*, 2015, **119**, 11099–11105.
28 J. Kong and S. Yu, *Acta Biochim Biophys Sin (Shanghai)*, 2007, **39**, 549–559.
29 P. Gagnon, R. Nian, D. Leong and A. Hoi, *J Chromatogr A*, 2015, **1395**, 136–142.
30 P. Bharmoria, A. A. Tietze, D. Mondal, T. S. Kang, A. Kumar and M. G. Freire, *Chem. Rev.*, 2024, **124**, 3037–3084, DOI: 10.1021/acs.chemrev.3c00551.
31 A. Sanchez-Fernandez, M. Basic, J. Xiang, S. Prevost, A. J. Jackson and C. Dicko, *J. Am. Chem. Soc.*, 2022, **144**, 23657–23667, DOI: 10.1021/jacs.2c11190.
32 N. N. Khechinashvili, J. Janin and F. Rodier, *Protein Sci*, 1995, **4**, 1315.
33 A. K. Upadhyay, A. Singh, K. J. Mukherjee and A. K. Panda, *Front Microbiol*, 2014, **5,** 486.
34 C. J. Roberts, *Curr Opin Biotechnol*, 2014, 30, 211–217.
35 J. Smiatek, *J Phys Chem B*, 2014, **118**, 771–782.
36 D. R. Canchi and A. E. García, *Annu Rev Phys Chem*, 2013, **64**, 273–293.
37 A. E. M. de Brito, A. Pessoa, A. Converti, C. de O. Rangel-Yagui, J. A. da Silva and A. C. Apolinário, *Mat Sci Eng C*, 2019, **98**, 524–534.
38 Kitchen, D. B., Decornez, H., Furr, J. R., & Bajorath, J., *Nature Rev Drug Disc*, 2004, **3**, 935-949.(CB-DOCK)
39 Erdi, M.; Ramesh, A.; Suja, V. C.; Zhang, S.; Mitragotri, S.; Singh, B. High Concentration Antibody Formulations Enabled via Thermostable Ionic Liquids. *Advanced Materials* **2026**, *38* (14), e11918. https://doi.org/10.1002/adma.202511918.
40 J. Zarzar, T. Khan, M. Bhagawati, B. Weiche, J. Sydow-Andersen and S. Alavattam, *mAbs*, 2023, **15**, 2211185, DOI: 10.1080/19420862.2023.2211185.
41 S. R. Wlodarczyk, T. A. Costa-Silva, A. Pessoa-Jr, P. Madeira and G. Monteiro, *Process Biochem*, 2019, **81**, 123–131.
42 E. Bahreini, K. Aghaiypour, R. Abbasalipourkabir, A. R. Mokarram, M. T. Goodarzi and M. Saidijam, *Nanoscale Res Lett*, 2014, **9**, 1–13.
43 Y. Liu, M. Grimm, W. tao Dai, M. chun Hou, Z. X. Xiao and Y. Cao, *Acta Pharmacol Sin*, 2020, **41**, 138–144.
44 R. Radha and S. N. Gummadi, *Protein Pept. Lett.*, 2019, **26**, 743–750. DOI: 10.2174/0929866526666190617092944
45 T. Costa-Silva, G. V. Ruiz-Lara, I. M. Costa, A. Pessoa Jr, and G. Monteiro, *ACS Pharmacol. Transl. Sci.*, 2025, **8**, 4371–4384
46 L. Huang, Y. Liu, Y. Sun, Q. Yan and Z. Jiang, *Appl. Environ. Microbiol.*, 2014, **80**, 1561–1569. https://doi.org/10.1016/j.ijbiomac.2016.11.115.
47 A. L. Stecher, P. Morgantetti de Deus, I. Polikarpov and J. Abrahão-Neto, *Pharm Acta Helv*, 1999, **74**, 1–9.
48 A. Sanchez-Fernandez, M. Basic, J. Xiang, S. Prevost, A. J. Jackson and C. Dicko, *J Am Chem Soc*, 2022, **144**, 23657–23667.
49 M. Bisht and P. Venkatesu, *New J Chem*, 2017, **41**, 13902–13911.
50 M. V. Quental, M. Caban, M. M. Pereira, P. Stepnowski, J. A. P. Coutinho, M. G. Freire, *Biotechnol. J.*, **2015**, 10, 1457–1466, DOI: 10.1002/biot.201500003.
51 O. S. Hammond, D. T. Bowron and K. J. Edler, *ACS Sus. Chem. Eng.*, 2014, 2, 2416–2425, DOI: 10.1021/sc500439w.
52 D. Dhiman, S. Mor, U. Fatima and P. Venkatesu, *Mol Pharm*, 2023, **20**, 3150–3159.
53 O. Trott and A. J. Olson, *J Comput Chem*, 2010, **31**, 455–461.
54 M. R. Almeida, R. O. Cristóvão, M. A. Barros, J. C. F. Nunes, R. A. R. Boaventura, J. M. Loureiro, J. L. Faria, M. C. Neves, M. G. Freire and V. C. Santos-Ebinuma, *Sci Rep*, 2021, **11**, 21529.
55 R. O. Cristóvão, M. R. Almeida, M. A. Barros, J. C. F. Nunes, R. A. R. Boaventura, J. M. Loureiro, J. L. Faria, M. C. Neves, M. G. Freire and V. C. Ebinuma-Santos, *RSC Adv*, 2020, **10**, 31205–31213.

Data availability statement

View Article Online
DOI: 10.1039/D6RE00047A

The data supporting this article have been included as part of the Supplementary Information.